# Constrained $\mathcal{H}_2/\mathcal{H}_\infty$ Control Design of Dynamic Virtual Power Plants via System Level Synthesis and Simple Pole Approximation

Zhong Fang
*University of Waterloo*
Waterloo, Canada
z4fang@uwaterloo.ca

Michael W. Fisher
*University of Waterloo*
Waterloo, Canada
michael.fisher@uwaterloo.ca

***Abstract*—Future power systems are expected to integrate an increasing share of non-synchronous distributed energy resources. This transition introduces significant challenges due to the variability of renewable energy sources and the operational limitations of individual devices. Designing optimal linear feedback controllers that achieve desired aggregate system behavior while respecting both state and input constraints is a critical and challenging task to support this transformation. In this paper, we propose a novel control framework for dynamic virtual power plants. Specifically, we consider a group of heterogeneous distributed energy resources that collectively deliver dynamic ancillary services, such as fast frequency and voltage regulation. Local linear state-feedback $\mathcal{H}_2/\mathcal{H}_\infty$ controllers are designed to optimally achieve the desired aggregate system behavior. System level synthesis is a recent technique that reparameterizes the optimal control problem as a convex program and has previously been combined with simple pole approximations to address infinite-dimensional challenges. This work extends the design framework to a multi-controller design that explicitly incorporates the physical and engineering constraints of each DVPP device, including state, input, and output limits, which also provides guaranteed suboptimality bounds and results in a convex and tractable semidefinite program for the control design. Finally, we demonstrate the effectiveness of our control strategy in a case study based on the IEEE nine-bus system.**

## I. Introduction

The shift from conventional synchronous machines to converter-interfaced distributed energy resources (DERs) is transforming the way essential grid services are provided. While synchronous machines have historically maintained frequency and voltage stability, future power systems must rely on power converters to perform these roles. This transition enables new control opportunities, such as fast, coordinated frequency and voltage regulation, but also introduces challenges, including cross-coupling effects, poorly damped oscillations, and reduced system robustness.

The concept of virtual power plants (VPPs) was introduced as early as 1997 to address this transition [1]. VPPs aggregate multiple distributed generators, each with individual operational constraints, to collectively achieve the controllability, visibility, and market participation of a traditional power plant [2]. Despite significant progress, both commercial implementations and much of the academic research to date have primarily focused on VPPs delivering static ancillary services, such as tracking predefined power and voltage reference signals [3].

This work investigates the concept of dynamic virtual power plants (DVPPs) composed of heterogeneous distributed energy resources, aimed at providing dynamic ancillary services beyond setpoint tracking. In contrast to existing VPPs, DVPPs can deliver fast frequency and voltage regulation through coordinated control of diverse devices. Heterogeneity is key to reliable dynamic ancillary services. A diverse group of devices, with varying capacities and response times, is necessary to provide these services across different power levels and time scales, as no single device can do so alone. However, previous efforts combining heterogeneous resources, such as hydropower with batteries or synchronous condensers with converter-based generation [4], have been highly customized and lack general applicability or optimal dynamic performance. Moreover, they do not enforce a desired aggregate system behavior. Here, we propose a novel multivariable control framework for DVPPs that simultaneously delivers multiple dynamic ancillary services while explicitly addressing device constraints and adapting to resource variations.

To propose this control design framework, the primary challenge is the nonconvexity of the controller design problem. One approach to address this is convex reparameterization, which changes the variables to make the optimization problem convex. A classical example is the Youla parametrization [5], while more recent methods include system level synthesis (SLS) [6] and input-output parametrization (IOP) [7]. Compared to Youla parametrization [8], both SLS and IOP offer advantages, such as directly parameterizing the control design using closed-loop system responses. This work focuses on SLS, as it is well-suited for state feedback design, whereas IOP is primarily used for output feedback.

Convex reparameterization yields tractable but infinite-dimensional control formulations, prompting the development of finite-dimensional approximations in SLS. While the finite impulse response (FIR) approximation [9] has been widely adopted by constraining all closed-loop poles to the origin, it presents several fundamental limitations. Beyond inducing infeasibility for stabilizable yet uncontrollable systems and

computational challenges in stiff dynamics, its imposed locality constraints prove particularly restrictive for networked systems with strong coupling, such as power systems. Furthermore, the resulting deadbeat control behavior, characterized by excessively large gains, significantly compromises robustness to disturbances. These limitations motivate the simple pole approximation (SPA) [10], which employs stable and distinct poles within the unit disk. This approach not only guarantees feasibility for stabilizable systems and avoids undesirable deadbeat behavior but also provides flexibility in incorporating prior knowledge of optimal pole locations. Importantly, as demonstrated in [11], SPA can handle state and input constraints in a non-conservative manner, establishing it as a more versatile framework for practical control applications.

This work develops a tractable control design framework for DVPPs that enables optimal $\mathcal{H}_2/\mathcal{H}_\infty$ model matching with certified suboptimality. The goal is to match a desired aggregate response while satisfying local constraints on each DER, enabling scalable, constraint-aware coordination of heterogeneous devices for dynamic ancillary services. We propose a hybrid formulation that combines frequency-domain and state-space representations. While SLS constraints remain affine in the frequency domain, we employ the Kalman-Yakubovich-Popov (KYP) lemma to express the $\mathcal{H}_2/\mathcal{H}_\infty$ objectives as LMIs in the state space. To do so, closed-loop responses are approximated using the simple pole method. Unlike finite-horizon approaches, our method avoids time-domain truncation and its associated limitations, resulting in a convex semidefinite program that is both efficient and accurate. The proposed hybrid domain method offers bounded suboptimality [12], handles state, input, output, and coupling constraints without conservatism, and avoids manual controller tuning. Its effectiveness is demonstrated in Section VI, where coordinated DER control enables grid-level frequency regulation.

The rest of this paper is structured as follows. Section II introduces the problem formulation. Section III provides a valuable state space realization of the closed-loop system. The main results on the novel control design method are shown in Section IV. The derivation of the control design methods is presented in Section V. A numerical example is provided in Section VI. Finally, Section VII offers concluding remarks.

*Notation:* The superscript "$\intercal$" and $\mathrm{Tr}\{\cdot\}$ denote the transpose and trace of a matrix, respectively. For a complex number $z$, let $\mathrm{Re}(z)$, $\mathrm{Im}(z)$, and $\overline{z}$ represent the real part, imaginary part, and complex conjugate of $z$. For any matrix $A$, We say a matrix $A$ is Schur if all of its eigenvalues have modulus less than one. A positive definite (semidefinite) matrix $P$ is denoted by $P \succ 0 (P \succeq 0)$. The set of real (symmetric) matrices of dimension $n \times m(n)$ is denoted by $\mathbb{R}^{n\times m}(\mathbb{S}^n)$. $0_n$ and $I_n$ are the $n \times n$ zero and identity matrices, and $n$ is often omitted if there is no ambiguity. For any set $S$, let $|S|$ be its cardinality (i.e., the number of elements it contains). Let $\mathcal{M}$ denote a collection of matrices $\{M_i\}_{i=1}^{l}$, define the block diagonal concatenation operator by $\mathcal{D}(\mathcal{M}) := \begin{bmatrix} M_1 & & \\ & \ddots & \\ & & M_\ell \end{bmatrix}$ where the off-diagonal entries are all zero, and define the block row concatenation operator by $\mathcal{R}(\mathcal{M}) := \begin{bmatrix} M_1 & \dots & M_l \end{bmatrix}$. The operator $\otimes$ denotes the Kronecker product between any two matrices. We denote the set of real, rational, strictly proper, and stable transfer function matrices as $\frac{1}{z}\mathcal{RH}_\infty$. For any stable transfer matrix $S \in \frac{1}{z}\mathcal{RH}_\infty$, let $\mathcal{J}(S)(k)$ denote its impulse response at time $k$. The convolution operator $\mathcal{C}(S)$ maps an input sequence $u(n)$ to an output sequence $y(n) = \sum_{k=1}^{\infty} \mathcal{J}(S)(k)u(n-k)$. And $\mathcal{J}_T(S)$ is a stacked vector of the first $T$ impulse responses, and $\mathcal{C}_T(S)$ is a lower-triangular block Toeplitz matrix formed from $\mathcal{J}(S)(k)$.

## II. Problem Statement and Background

### A. DVPP Control Setup

TABLE I
List of Notation for the DVPP Control Setup

| Description | Symbol |
|---|---|
| Set of DVPP devices | $\mathcal{N}$ |
| DVPP devices index | $i$ |
| Measured bus frequency deviation | $\Delta f$ |
| Measured bus voltage magnitude deviation | $\Delta v$ |
| Active power deviation output of device $i$ | $\Delta p_i$ |
| Reactive power deviation output of device $i$ | $\Delta q_i$ |
| Aggregate active power deviation output of the DVPP | $\Delta p_{\mathrm{agg}}$ |
| Aggregate reactive power deviation output of the DVPP | $\Delta q_{\mathrm{agg}}$ |
| Desired active power deviation output of the DVPP | $\Delta p_{\mathrm{des}}$ |
| Desired reactive power deviation output of the DVPP | $\Delta q_{\mathrm{des}}$ |
| Local closed-loop transfer matrix of device $i$ | $T_i(z)$ |
| Desired MIMO transfer matrix of the DVPP | $T_{\mathrm{des}}(z)$ |
| Desired DVPP transfer function for the f-p channel | $T_{\mathrm{des}}^{\mathrm{fp}}(z)$ |
| Desired DVPP transfer function for the v-q channel | $T_{\mathrm{des}}^{\mathrm{vq}}(z)$ |

Consider a DVPP control framework comprising a collection of heterogeneous DERs [13]. All units within the DVPP are assumed to be connected to the same bus of the transmission grid, where they receive common input signals, the measured bus frequency deviation $\Delta f$ and voltage magnitude deviation $\Delta v$. The active and reactive power deviation output of each device $i$, namely $\Delta p_i$ and $\Delta q_i$, respectively (deviating from the respective power set point), sum up to the aggregate active and reactive power deviation output of the DVPP, namely $\Delta p_{\mathrm{agg}}$ and $\Delta q_{\mathrm{agg}}$ , respectively, i.e.,

$$\begin{bmatrix} \Delta p_{\mathrm{agg}} \\ \Delta q_{\mathrm{agg}} \end{bmatrix} = \sum_{i\in\mathcal{N}} \begin{bmatrix} \Delta p_i \\ \Delta q_i \end{bmatrix}. \tag{1}$$

The local closed-loop transfer matrices $T_i(z) \in \mathbb{R}^{2\times 2}$ associated with the devices $i \in \mathcal{N}$ can be systematically shaped through the design of suitable feedback controllers. More details can be found in Section II-B.

The aggregate behavior of the DVPP is characterized by

$$\begin{bmatrix} \Delta p_{\mathrm{agg}}(z) \\ \Delta q_{\mathrm{agg}}(z) \end{bmatrix} = \sum_{i\in\mathcal{N}} T_i(z) \begin{bmatrix} \Delta f(z) \\ \Delta v(z) \end{bmatrix}. \tag{2}$$

To replicate the ancillary services traditionally provided by synchronous generators in transmission systems, a decoupled

f-p and v-q dynamic response is prescribed for the aggregate DVPP as a desired diagonal MIMO transfer matrix as

$$\begin{bmatrix}\Delta p_{\mathrm{des}}(z)\\ \Delta q_{\mathrm{des}}(z)\end{bmatrix} = \underbrace{\begin{bmatrix}T_{\mathrm{des}}^{\mathrm{fp}}(z) & 0\\ 0 & T_{\mathrm{des}}^{\mathrm{vq}}(z)\end{bmatrix}}_{=:\,T_{\mathrm{des}}(z)} \begin{bmatrix}\Delta f(z)\\ \Delta v(z)\end{bmatrix}. \tag{3}$$

The DVPP control design problem is to find local controllers for the controllable devices $\mathcal{C}$, such that the following aggregation condition holds:

$$\sum_{i\in\mathcal{N}} T_i(z) \stackrel{!}{=} T_{\mathrm{des}}(z) \tag{4}$$

where "$\stackrel{!}{=}$" indicates that the terms on the left hand side of the equality achieve the right side as closely as possible.

During control design, it is essential to respect each device's physical limits, such as bandwidth, power availability, and current capacity, under normal operation. Moreover, the DVPP must be sufficiently diverse to span all relevant time scales and power levels. We assume the desired reference $T_{\mathrm{des}}$ is specified by the system operator so that it is achievable by the ensemble, guarantees closed-loop stability, and remains robust to grid uncertainties and parameter variations.

### B. $\mathcal{H}_2/\mathcal{H}_\infty$ Control Design

To find local feedback controls for the devices $\mathcal{N}$ to ensure their closed-loop transfer matrices $T_i$ satisfy the aggregation condition (4), we consider the linear time-invariant (LTI) systems in discrete time described by the following state space representation:

$$\begin{aligned} x_i^{k+1} &= A_i x_i^k + B_i u_i^k + \hat{B}_i w^k\\ y_i^k &= C_i x_i^k \end{aligned} \tag{5}$$

where $x_i^k \in \mathbb{R}^n$, $u_i^k \in \mathbb{R}^p$, $y_i^k \in \mathbb{R}^m$ are the states, controller signal, and performance output vectors at time step $k$ for each device $i \in \mathcal{N}$, respectively, note that all devices are subject to a common disturbance input $w^k \in \mathbb{R}^q$ as they are connected in parallel. It will be useful to define the signal $v_i^k = \hat{B}_i w^k$.

Consider linear state feedback control laws of the form $u_i(z) = K_i(z)x_i(z)$ for each device $i \in \mathcal{N}$, where $K_i(z)$ is a dynamic controller. The closed-loop transfer function mapping disturbance $w$ to each output $y_i$ is $T_{w\to y_i}(z)$, and $T_{w\to u_i}(z)$, $T_{v_i\to x_i}(z)$, and $T_{v_i\to u_i}(z)$ are defined analogously. And $T_{\mathrm{des}}(z)$ in (3) is the desired closed-loop transfer function for model matching control design.

The goal of this paper is to design local controllers $K_i(z)$ such that their collection is a solution to the following mixed $\mathcal{H}_2/\mathcal{H}_\infty$ model matching problem:

$$\begin{aligned} \underset{\{K_i(z)\}_{i\in\mathcal{N}}}{\text{minimize}} \quad & \left\| \begin{bmatrix}Q & 0\\ 0 & R\end{bmatrix} \begin{bmatrix}\sum_{i\in\mathcal{N}} T_{w\to y_i}(z) - T_{\mathrm{des}}(z)\\ \sum_{i\in\mathcal{N}} T_{w\to u_i}(z)\end{bmatrix} \right\|_{\mathcal{H}_2/\mathcal{H}_\infty}\\ \text{subject to} \quad & T_{v_i\to x_i}(z), T_{v_i\to u_i}(z) \in \mathcal{R}_i,\ \forall i \in \mathcal{N} \end{aligned} \tag{6}$$

where the mixed $\mathcal{H}_2/\mathcal{H}_\infty$ norm is given by $\|T\|_{\mathcal{H}_2/\mathcal{H}_\infty} = \|T\|_{\mathcal{H}_2} + \lambda\|T\|_{\mathcal{H}_\infty}$ for some constant $\lambda \in [0,\infty]$. The constant matrices $Q$ and $R$ represent the weights on output and input, respectively. $\mathcal{R}_i$ is the Hardy space of real, rational, strictly proper, and stable transfer functions for device $i$, that additionally satisfy time-dependent constraints:

i) The trajectories of the *states, inputs, and outputs* induced by known disturbance signals $w^{0:T}$ over a finite horizon $T$ are given by

$$x_i^{0:T} = \mathcal{C}^{0:T}[T_{v_i\to x_i}(z)]v_i^{0:T}, \tag{7}$$
$$u_i^{0:T} = \mathcal{C}^{0:T}[T_{v_i\to u_i}(z)]v_i^{0:T}, \tag{8}$$
$$y_i^{0:T} = \mathcal{C}^{0:T}[T_{v_i\to y_i}(z)]v_i^{0:T}, \tag{9}$$

and are required to satisfy the prescribed bounds $m_{x,i}$, $m_{u,i}$, and $m_{y,i}$, respectively.

ii) *Steady state gain* in response to a unit step input exists and can be computed using the final value theorem as

$$y_i^\infty = \lim_{z\to 1} T_{w\to y_i}(z) \tag{10}$$

for all devices $i \in \mathcal{N}$. Note that (6) is nonconvex in $\{K_i(z)\}_{i\in\mathcal{N}}$ since $T_{w\to y_i}(z)$ and $T_{w\to u_i}(z)$ are, so this problem is challenging to solve in this form.

Using SLS, (6)-(10) can be equivalently reformulated as follows (we refer the reader to [6] for further details about SLS)

$$\underset{\{\Phi_{x,i},\Phi_{u,i}\}_{i\in\mathcal{N}}}{\text{minimize}} \quad \left\| \begin{bmatrix}Q & 0\\ 0 & R\end{bmatrix} \begin{bmatrix}\sum_{i\in\mathcal{N}} \tilde{\Phi}_{x,i} - T_{\mathrm{des}}\\ \sum_{i\in\mathcal{N}} \tilde{\Phi}_{u,i}\end{bmatrix} \right\|_{\mathcal{H}_2/\mathcal{H}_\infty} \tag{11a}$$

$$\text{subject to} \quad (zI - A_i)\Phi_{x,i}(z) - B_i\Phi_{u,i}(z) = I, \tag{11b}$$

$$\Phi_{x,i}(z), \Phi_{u,i}(z) \in \frac{1}{z}\mathcal{R}\mathcal{H}_\infty \tag{11c}$$

$$x_i^k = \sum_{l=0}^{k} \mathcal{J}^{k-l}\left[\Phi_{x,i}\right]\hat{B}_i w^l \le m_{x,i} \tag{11d}$$

$$u_i^k = \sum_{l=0}^{k} \mathcal{J}^{k-l}\left[\Phi_{u,i}\right]\hat{B}_i w^l \le m_{u,i} \tag{11e}$$

$$y_i^k = \sum_{l=0}^{k} C_i\mathcal{J}^{k-l}\left[\Phi_{x,i}\right]\hat{B}_i w^l \le m_{y,i} \tag{11f}$$

$$y_i^T = C_i\Phi_{x,i}(1)\hat{B}_i,\ \forall i \in \mathcal{N},\ \forall k \in [0,T] \tag{11g}$$

where $\Phi_{x,i}(z)$ and $\Phi_{u,i}(z)$ are the design variables, corresponding to the closed-loop transfer functions $T_{v_i\to x_i}(z)$ and $T_{v_i\to u_i}(z)$, respectively. We define $\tilde{\Phi}_{x,i}(z) = T_{w\to y_i}(z) = C_i\Phi_{x,i}(z)\hat{B}_i$ and $\tilde{\Phi}_{u,i}(z) = T_{w\to u_i}(z) = \Phi_{u,i}(z)\hat{B}_i$. The constraint (11c) guarantees the stability and well-posedness of the closed-loop system, while (11b) imposes an additional affine constraint required by SLS. By expressing the relevant transfer functions using the SLS variables and representing convolution operators through impulse responses, state, input and output constraints (7)–(9) naturally lead to (11d)–(11f) at time $k$. Furthermore, the steady-state gain constraint in (10) is captured by (11g). The controller for each device can be recovered locally as $K_i(z) = \Phi_{u,i}(z)\Phi_{x,i}^{-1}(z)$ based only on local information, i.e., $\Phi_{x,i}(z)$ and $\Phi_{u,i}(z)$. Note that (11) becomes convex under this reparameterization, although still infinite-dimensional since $\Phi_{x,i}(z)$ and $\Phi_{u,i}(z)$ lie in the

infinite dimensional function space $\mathcal{RH}_\infty$.

To circumvent this issue, [11] approximates the closed-loop transfer functions using a finite selection of simple stable poles $\{\mathcal{P}_i\}_{i\in\mathcal{N}}$, closed under complex conjugation, as

$$\Phi_{x,i}(z) = \sum_{p\in\mathcal{P}_i} G_{p,i}\frac{1}{z-p},\ \Phi_{u,i}(z) = \sum_{p\in\mathcal{P}_i} H_{p,i}\frac{1}{z-p} \quad (12)$$

where $G_{p,i}$ and $H_{p,i}$ are (complex) coefficient matrices for each $p\in\mathcal{P}_i$ and $i\in\mathcal{N}$. This simple pole approximation (SPA) renders (11) finite dimensional. In [12], a hybrid state space and frequency domain control design framework is proposed to address the optimization after (11) and (12) as a semidefinite program, and the suboptimality of the solution of SLS with SPA will tend to zero as the number of poles approaches infinity. In this paper, we extend this framework to the multi-controller design problem for DVPP control.

For SPA, since $\Phi_{x,i}(z)$ and $\Phi_{u,i}(z)$ are real, it is straightforward to show that for any real pole $p$, $G_{p,i}$ and $H_{p,i}$ are real, and for any complex pole $p$, $G_{\overline{p},i} = \overline{G_{p,i}}$ and $H_{\overline{p},i} = \overline{H_{p,i}}$. Let $\mathcal{P}_{r,i}$ denote the real poles in $\mathcal{P}_i$, and let $\mathcal{P}_{c,i}$ denote its complex poles in device $i\in\mathcal{N}$. Then $\mathcal{P}_i = \mathcal{P}_{r,i}\cup\mathcal{P}_{c,i}$.

## III. Closed-Loop Realization

To derive the proposed hybrid state space and frequency domain control design method, we will require state space realizations of the closed-loop transfer functions. In this section, we propose novel state space realizations of the entire closed-loop dynamics in DVPP based on the simple pole approximation.

For any $p\in\mathcal{P}_{c,i}$, its conjugate $\overline{p}$ is also in $\mathcal{P}_{c,i}$, their corresponding coefficient matrices are:

$$\begin{aligned} &G_{p,i} = \mathrm{Re}(G_{p,i}) + \mathrm{Im}(G_{p,i})j, G_{\overline{p},i} = \mathrm{Re}(G_{p,i}) - \mathrm{Im}(G_{p,i})j,\\ &H_{p,i} = \mathrm{Re}(H_{p,i}) + \mathrm{Im}(H_{p,i})j, H_{\overline{p},i} = \mathrm{Re}(H_{p,i}) - \mathrm{Im}(H_{p,i})j. \end{aligned} \quad (13)$$

For simplicity, the subscript $i$ in $G_{p,i}$ and $H_{p,i}$ is omitted whenever it does not cause ambiguity.

We first find the realization of the individual closed-loop transfer functions $\tilde{\Phi}_{x,i}(z)$ and $\tilde{\Phi}_{u,i}(z)$ for each device $i\in\mathcal{N}$. To do so, for each complex conjugate pair $p,\overline{p}\in\mathcal{P}_{c,i}$, define the matrix

$$M(p) = \begin{bmatrix} \mathrm{Re}(p) & \mathrm{Im}(p) \\ -\mathrm{Im}(p) & \mathrm{Re}(p)\end{bmatrix},$$

and let $\mathcal{M}_{c,i}$ be the collection of $M(p)$ for all such complex conjugate pairs. Let $\mathcal{M}_{r,i}$ be the collection of each scalar matrix $p$ for all $p\in\mathcal{P}_{r,i}$. Then we can define

$$\begin{aligned} \overline{A}_i &= \begin{bmatrix}\mathcal{D}(\mathcal{M}_{r,i}) & \\ & \mathcal{D}(\mathcal{M}_{c,i})\end{bmatrix}\otimes I,\\ \overline{B}_i &= \big[\underbrace{I\ \cdots\ I}_{|\mathcal{P}_{r,i}|}\ \underbrace{2I\ 0\ \cdots\ 2I\ 0}_{|\mathcal{P}_{c,i}|}\big]^\intercal \hat{B}_i. \end{aligned}$$

Next, for each complex conjugate pair $p,\overline{p}\in\mathcal{P}_{c,i}$, define the matrices

$$G(p) = \begin{bmatrix}\mathrm{Re}(G_p) & \mathrm{Im}(G_p)\end{bmatrix}, H(p) = \begin{bmatrix}\mathrm{Re}(H_p) & \mathrm{Im}(H_p)\end{bmatrix},$$

and let $\mathcal{G}_{c,i}$ and $\mathcal{H}_{c,i}$ be the collection of $G(p)$ and $H(p)$, respectively, for all such complex conjugate pairs. Let $\mathcal{G}_{r,i}$ and $\mathcal{H}_{r,i}$ be the collection of $G_p$ and $H_p$, respectively, for each $p\in\mathcal{P}_{r,i}$. Then we define

$$\begin{aligned} \overline{C}_{x,i} &= C\begin{bmatrix}\mathcal{R}(\mathcal{G}_{r,i}) & \mathcal{R}(\mathcal{G}_{c,i})\end{bmatrix},\\ \overline{C}_{u,i} &= \begin{bmatrix}\mathcal{R}(\mathcal{H}_{r,i}) & \mathcal{R}(\mathcal{H}_{c,i})\end{bmatrix}. \end{aligned}$$

It is straightforward to verify that $(\overline{A}_i,\overline{B}_i,\overline{C}_{x,i},0)$ is a real state space realization of $\tilde{\Phi}_{x,i}(z)$, and that $(\overline{A}_i,\overline{B}_i,\overline{C}_{u,i},0)$ is a real state space realization of $\tilde{\Phi}_{u,i}(z)$ from [12].

Let $(A_{\mathrm{des}},B_{\mathrm{des}},C_{\mathrm{des}},0)$ be any real state space realization of $T_{\mathrm{des}}$. Now we can represent the transfer function in the objective (11a) using the following real state space realization

$$\begin{aligned} \tilde{A} &= \begin{bmatrix}\overline{A}_1 & 0 & \cdots & 0 & 0\\ 0 & \overline{A}_2 & \cdots & 0 & 0\\ \vdots & \vdots & \ddots & \vdots & \vdots\\ 0 & 0 & \cdots & \overline{A}_{|\mathcal{N}|} & 0\\ 0 & 0 & \cdots & 0 & A_{\mathrm{des}}\end{bmatrix},\ \tilde{B} = \begin{bmatrix}\overline{B}_1\\ \overline{B}_2\\ \vdots\\ \overline{B}_{|\mathcal{N}|}\\ B_{\mathrm{des}}\end{bmatrix},\\ \tilde{C} &= \begin{bmatrix}Q\overline{C}_{x,1} & Q\overline{C}_{x,2} & \cdots & Q\overline{C}_{x,|\mathcal{N}|} & -QC_{\mathrm{des}}\\ R\overline{C}_{u,1} & R\overline{C}_{u,2} & \cdots & R\overline{C}_{u,|\mathcal{N}|} & 0\end{bmatrix}. \end{aligned} \quad (14)$$

which satisfies

$$\tilde{C}(zI-\tilde{A})^{-1}\tilde{B} = \begin{bmatrix}Q & 0\\ 0 & R\end{bmatrix}\begin{bmatrix}\sum_{i\in\mathcal{N}}\tilde{\Phi}_{x,i} - T_{\mathrm{des}}\\ \sum_{i\in\mathcal{N}}\tilde{\Phi}_{u,i}\end{bmatrix} =: \Phi(z). \quad (15)$$

Thus, we have obtained an equivalent state space representation of the closed-loop transfer function $\Phi(z)$, which will be used to develop our novel control design method. Note that for a fixed collection of simple poles $\cup_{i\in\mathcal{N}}\mathcal{P}_i$, as used for SPA, $\tilde{A}$ and $\tilde{B}$ are constant matrices, and $\tilde{C}$ is an affine function of all of the variable coefficients $G_{p,i}$ and $H_{p,i}$.

## IV. Main Results

In this section we present our hybrid state space and frequency domain DVPP control design method which does not require any finite time horizon approximations for computing the $\mathcal{H}_2$ and $\mathcal{H}_\infty$ norms of the closed-loop transfer functions. As a result, it has reduced suboptimality, better performance, and lower computational cost compared to prior work [11]. The full derivation of the method is presented in Section V, but the key idea is to use the state space realizations provided in Section III together with the KYP lemma to derive an equivalent state space representation of the $\mathcal{H}_2$ and $\mathcal{H}_\infty$ norms of the closed-loop transfer functions as LMIs. However, the additional SLS constraints required for the SLS formulation no longer remain affine if we represent them in state space, so we choose to retain their frequency domain representation. Combining these two representations, we obtain the following control design formulation for the solution to (11) with the SPA (12) ($\star$ indicates symmetric blocks)

$$\underset{K_1,K_2,Z,\{G_{p,i},H_{p,i}\}_{i\in\mathcal{N}},\gamma_1,\gamma_2}{\text{minimize}} \quad \gamma_1+\lambda\gamma_2 \quad (16a)$$

$$\text{subject to} \quad \begin{bmatrix}K_1 & \star & \star\\ \tilde{A}^\intercal K_1 & K_1 & \star\\ \tilde{B}^\intercal K_1 & 0 & \gamma_1 I\end{bmatrix} \succ 0 \quad (16b)$$

$$\begin{bmatrix} K_1 & \star & \star \\ 0 & I & \star \\ \tilde{C}(G_{p,i}, H_{p,i}) & 0 & Z \end{bmatrix} \succ 0 \quad (16c)$$

$$\mathrm{Tr}(Z) < \gamma_1 \quad (16d)$$

$$\begin{bmatrix} K_2 & \star & \star & \star \\ 0 & \gamma_2 I & \star & \star \\ K_2\tilde{A} & K_2\tilde{B} & K_2 & \star \\ \tilde{C}(G_{p,i}, H_{p,i}) & 0 & 0 & \gamma_2 I \end{bmatrix} \succ 0 \quad (16e)$$

$$\sum_{p\in\mathcal{P}_i} G_{p,i} = I, \qquad \forall i \in \mathcal{N} \quad (16f)$$

$$(pI - A_i)\, G_{p,i} - B_i H_{p,i} = 0, \quad \forall p \in \mathcal{P}_i, \quad \forall i \in \mathcal{N} \quad (16g)$$

$$(19), (20), (21), (22), \quad \forall k \in [0, T], \ \forall i \in \mathcal{N} \quad (16h)$$

where $K_1, K_2 \in \mathbb{S}^{n\times(|\mathcal{P}||\mathcal{N}|)}$, $Z \in \mathbb{S}^m$, and $\gamma_1, \gamma_2$ are scalar variables that represent the $\mathcal{H}_2$ and $\mathcal{H}_\infty$ norms of the closed-loop transfer functions, respectively. Recall that $\tilde{A}$, $\tilde{B}$, and $\tilde{C}$ were defined in (14), but we write $\tilde{C} = \tilde{C}(G_{p,i}, H_{p,i})$ to emphasize that $\tilde{C}$ is an affine function of the coefficients $G_{p,i}$ and $H_{p,i}$ for all $p \in \mathcal{P}_i$.

Since, using SPA, we have already selected the closed-loop poles $\cup_{i\in\mathcal{N}}\mathcal{P}_i$, $\tilde{A}$ and $\tilde{B}$ are constant matrices, along with $A$, $B$, and $C$. Thus, the objective (16a) and the constraint (16g) are linear, the constraints (16f) and (22) are affine, the constraints (19)-(21) are affine inequalities since the disturbance $w$ is known and the poles are fixed, so these are affine in the decision variables $G_{p,i}$ and $H_{p,i}$, and the constraints (16b)-(16e) are LMIs in the decision variables. Therefore, overall (16) is a convex semidefinite program (SDP) that can be solved efficiently. Note that the state space realizations of the closed-loop transfer functions from Section III were deliberately constructed to ensure that the constraints (16b)-(16e) become LMIs rather than nonconvex bilinear matrix inequalities by including all the decision variables $G_{p,i}, H_{p,i}$ in $\tilde{C}$ and leaving $\tilde{A}, \tilde{B}$ as constant matrices.

As we will see in Section V, the objective (16a) and constraints (16b)-(16e) are derived from a state space representation, whereas the constraints (16f)-(16h) represent the SLS constraints in the frequency domain, which together yield a truly hybrid control design. Thus the hybrid state space and frequency domain control design method [12] is extended to multi controller systems and the error of finite time horizon approximation in [11] is thus entirely eliminated by the proposed design approach. As a result, for the Archimedes spiral pole selection proposed in [10], the suboptimality bound from [11, Corollary 1] applies immediately to this new design method (16), thus the suboptimality will tend to zero as the number of poles approaches infinity. As we will see in the numerical example in Section VI, even a small number of poles can often result in low suboptimality, and thus good performance, in practice.

## V. Control Design Derivation

This section presents the derivation of our control design optimization problem (16). We begin with the problem formulation of SLS (11) together with SPA (12). First we will derive the representation of the SLS constraints (11b) for SPA, and then we will derive the state space representation of the objective function (11a).

For the SLS constraint (11b), substituting in the SPA (12) and matching coefficients of $\frac{1}{z-p}$ for each pole $p \in \mathcal{P}_i$ since these functions are linearly independent, we obtain

$$I = \sum_{p\in\mathcal{P}_{r,i}} G_{p,i} + 2\sum_{p\in\mathcal{P}_{c,i}} \mathrm{Re}(G_{p,i}) = \sum_{p\in\mathcal{P}_i} G_{p,i} \quad (17)$$

for each $i \in \mathcal{N}$,

$$0 = (pI - A_i)\, G_{p,i} - B_i H_{p,i} \quad (18)$$

for each $i \in \mathcal{N}$ and $p \in \mathcal{P}_i$. Thus, the SLS constraint (11b) with the SPA (12) can be equivalently represented using (17)-(18).

Then, we address the design constraints on the state, input, output, and steady-state behavior using SPA. By [11], We denote the impulse response of $\Phi_{x,i}$ and $\Phi_{u,i}$ at time step $k$ as $\mathcal{J}^k[\Phi_{x,i}] := \sum_{p\in\mathcal{P}_i} G_{p,i} p^{k-1}$ and $\mathcal{J}^k[\Phi_{u,i}] := \sum_{p\in\mathcal{P}_i} H_{p,i} p^{k-1}$, respectively. Thus we have

$$\sum_{l=0}^{k}\sum_{p\in\mathcal{P}_i} G_{p,i} p^{k-l-1}\hat{B}_i w^l \le m_{x,i} \quad (19)$$

$$\sum_{l=0}^{k}\sum_{p\in\mathcal{P}_i} H_{p,i} p^{k-l-1}\hat{B}_i w^l \le m_{u,i} \quad (20)$$

$$\sum_{l=0}^{k}\sum_{p\in\mathcal{P}_i} p^{k-l-1} C_i G_{p,i}\hat{B}_i w^l \le m_{y,i} \quad (21)$$

$$C_i \sum_{p\in\mathcal{P}_i} G_{p,i}\frac{1}{1-p}\hat{B}_i = y_i^T. \quad (22)$$

Next, we will express the $\mathcal{H}_2$ and $\mathcal{H}_\infty$ norms of the closed-loop transfer functions from the objective function (11a) using a state space representation. To do so, we begin with the real state space realization $(\tilde{A}, \tilde{B}, \tilde{C}, 0)$ from (14), which is a realization of the closed-loop transfer function $\Phi(z)$ by (15). In order to calculate the objective (11a), we need to express $\|\Phi(z)\|_{\mathcal{H}_2}$ and $\|\Phi(z)\|_{\mathcal{H}_\infty}$ in terms of LMIs using a state space representation. To accomplish this, we apply the KYP lemma to obtain bounds on the $\mathcal{H}_2$ and $\mathcal{H}_\infty$ norms of our state space representation $(\tilde{A}, \tilde{B}, \tilde{C}, 0)$. This yields the following result from [14, Section 4.6]

*Theorem 1:* For the transfer function $\Phi(z) = \tilde{C}(zI - \tilde{A})^{-1}\tilde{B}$, if $\tilde{A}$ is Schur then the following statements hold.

(1) $\|\Phi(z)\|_{\mathcal{H}_2} < \gamma_1$ if and only if there exist $K_1 \in \mathbb{S}^{n\times(|\mathcal{P}||\mathcal{N}|)}$, $Z \in \mathbb{S}^m$, such that $\mathrm{Tr}(Z) < \gamma_1$ and

$$\begin{bmatrix} K_1 & K_1\tilde{A} & K_1\tilde{B} \\ \tilde{A}^\intercal K_1 & K_1 & 0 \\ \tilde{B}^\intercal K_1 & 0 & \gamma_1 I \end{bmatrix} \succ 0, \quad \begin{bmatrix} K_1 & 0 & \tilde{C}^\intercal \\ 0 & I & 0 \\ \tilde{C} & 0 & Z \end{bmatrix} \succ 0. \quad (23)$$

(2) $\|\Phi(z)\|_{\mathcal{H}_\infty} < \gamma_2$ if and only if there exists $K_2 \in \mathbb{S}^{n\times(|\mathcal{P}||\mathcal{N}|)}$,

$$\begin{bmatrix} K_2 & 0 & \tilde{A}^\intercal K_2 & \tilde{C}^\intercal \\ 0 & \gamma_2 I & \tilde{B}^\intercal K_2 & 0 \\ K_2\tilde{A} & K_2\tilde{B} & K_2 & 0 \\ \tilde{C} & 0 & 0 & \gamma_2 I \end{bmatrix} \succ 0. \quad (24)$$

Note that $\tilde{A}$ is Schur by construction because its eigenvalues consist of the poles $\mathcal{P}$ from SPA, which all lie inside the unit disk, so the assumptions of Theorem 1 are automatically satisfied. To use Theorem 1 to reexpress the objective function (11a), we note that

$$\min_{\Phi(z)\in\frac{1}{z}\mathcal{R}\mathcal{H}_\infty} \|\Phi(z)\|_{\mathcal{H}_2} + \lambda\|\Phi(z)\|_{\mathcal{H}_\infty}$$

is equivalent to

$$\min_{\gamma_1,\gamma_2,\Phi(z)\in\frac{1}{z}\mathcal{R}\mathcal{H}_\infty} \gamma_1 + \lambda\gamma_2 \tag{25a}$$

$$\text{s.t.} \quad \|\Phi(z)\|_{\mathcal{H}_2} < \gamma_1 \tag{25b}$$

$$\|\Phi(z)\|_{\mathcal{H}_\infty} < \gamma_2 \tag{25c}$$

since the two inequalities $\|\Phi(z)\|_{\mathcal{H}_2} < \gamma_1$ and $\|\Phi(z)\|_{\mathcal{H}_\infty} < \gamma_2$ will become tight at optimality. Now we can apply Theorem 1 to (25) to express the objective function (11a) equivalently in terms of LMIs. Thus, combining (23), (24), (25a), and (17)-(11), we arrive at the final control design optimization problem (16), which is equivalent to (11) with the SPA (12).

## VI. Test Case

To demonstrate the effectiveness of the proposed control design, we investigate a multivariable DVPP setup that replaces the fast frequency and voltage control traditionally provided by a thermal-based generator. The DVPP consists of an aggregation of DERs, including wind turbines (WTs), photovoltaics (PVs), and energy storage systems (ESs), which collectively provide fast frequency and voltage regulation services to the power grid. Specifically, we consider the IEEE 9-bus power system [15], a benchmark network comprising nine nodes, three synchronous generators, three loads, six transmission lines, and three transformers. In our setup, the thermal-based power plant at bus 3 is replaced by a DVPP, which includes a wind power plant, a PV system, and a battery energy storage system (BESS). The DVPP is designed to replicate the active power–frequency (f-p) and reactive power–voltage (v-q) control characteristics of the original thermal unit. To assess system performance, we consider a disturbance from a step change in the load.

For individual DERs, the continuous-time model in [13] shown here

$$\begin{aligned} \dot{x}_{pll} &= v^q \\ \dot{\theta}_{pll} &= k_{p,pll}v^q + k_{i,pll}x_{pll} \\ C\dot{v} &= -C\omega^* J_2 v + i_s - i \\ L\dot{i}_s &= -\left(L\omega^* J_2 + RI_2\right) i_s + v_s - v \end{aligned} \tag{26}$$

is normalized to define $c_d$ and $c_q$. The outputs are the active and reactive power injections. Key model parameters include the phase locked loop gains $k_{p,\text{pll}}$ and $k_{i,\text{pll}}$, the sampling time $h$, and the time constants $\tau_d$ and $\tau_q$ associated with the $d$- and $q$-axis current control loops, where we set $k_{i,\text{pll}} = 1700, k_{p,\text{pll}} = 150$ and $h = 0.0167$ in the simulation process. The parameter $\tau_i$ is the time constant of each DER and is equal to 1.5, 0.6 and 0.2 seconds for WT, PV and ES, respectively.

In addition, we want to substitute the services of the thermal-based power plant, and specify a f-p and v-q control as

$$\begin{bmatrix}\Delta p \\ \Delta q\end{bmatrix} = \begin{bmatrix}\frac{-1.1052}{z-0.944} & \\ & \frac{-1.1389}{z-0.944}\end{bmatrix}\begin{bmatrix}\Delta f \\ \Delta v\end{bmatrix}, \tag{27}$$

then we employ the $\mathcal{H}_2/\mathcal{H}_\infty$ matching control method in the outer control loop of each grid-side converter to match the desired accumulated by closed-loop dynamics of the DVPP 3 devices. We now aim to regulate the entire reference current to participate in the desired f-p and v-q control of DVPP 3 in (27). In this regard, we consider the previous converter model in (26), as well as the active and reactive power outputs as our plant model for control design.

For the control design, we choose $Q = I_2$, $R = 0.01I_2$, and $\lambda = 0.5$. For the SPA pole selection $\mathcal{P}$, we set the maximum number of closed-loop poles at $l = 15$. To form $\mathcal{P}$ we first incorporate the plant poles and the poles of the desired transfer function. The remaining poles are chosen along an Archimedes spiral as in [10]. We solve the SDP for the control design using MOSEK [16] in conjunction with YALMIP [17] in MATLAB.

The step responses for the desired transfer function in (27) and the aggregate response of all DVPP devices are shown in Fig. 1, where the DVPP output almost perfectly matches the desired response, demonstrating the extraordinary performance of the DVPP control design. Fig. 2 depicts the individual step responses of WT, PV, and ES to a unit disturbance. In the active-power plots (left), storage delivers a fast, brief pulse, PV provides a moderate sustained adjustment, and wind ramps slowly to the largest offset. In the reactive-power plots (right), storage is again fastest, PV is intermediate, and wind is slowest with the highest magnitude. Together, these complementary dynamics ensure that the aggregate DVPP can provide fast initial support via storage, sustained correction via PV, and long-term compensation via wind, which demonstrates the overall system's benefits arising from DER heterogeneity.

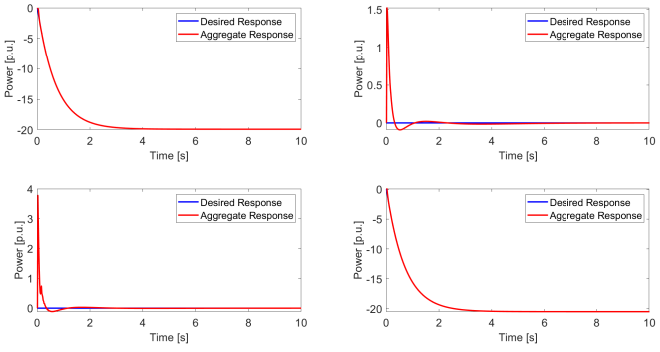


Fig. 1. Aggregate DVPP step response

Fig. 3 plots each device's apparent power output (solid) alongside its limit (dashed). Following a small disturbance, all devices exhibit only minor transients and remain strictly within their apparent-power bounds, confirming that the imposed constraints are satisfied.

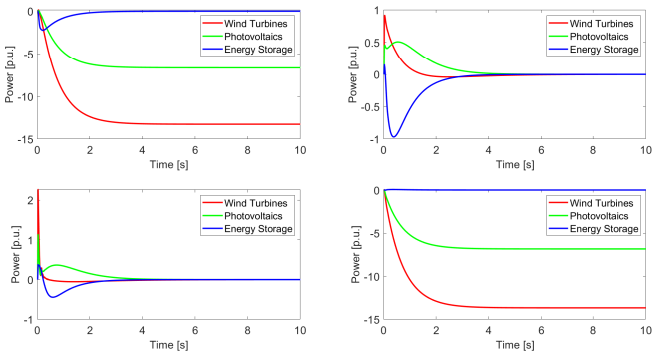


Fig. 2. Individual step response of each device

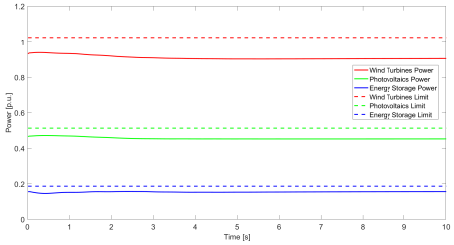


Fig. 3. Individual device apparent power disturbance responses

## VII. Conclusion

We have presented a tractable control framework for DVPPs that rigorously addresses the joint challenges of renewable variability and device-level constraints. By extending SLS with SPA to a multi-controller setting, our method yields a convex SDP whose solutions come with guaranteed suboptimality bounds. Local linear state-feedback $\mathcal{H}_2/\mathcal{H}_\infty$ controllers synthesized in this way ensure that the aggregate DVPP response closely matches a desired reference model while enforcing state, input, and output limits on each DER. A comprehensive case study on the IEEE nine-bus system demonstrates the efficacy of our approach. The results confirm that heterogeneous converter-interfaced DERs can be coordinated to deliver reliable frequency and voltage regulation in aggregate to the power grid while respecting individual device limitations. Future work will focus on developing distributed and scalable solvers for real-time implementation across geographically dispersed DERs and extending the proposed framework in other control policies such as output feedback control.

## References


[1] S. Awerbuch and A. Preston, *The virtual utility: Accounting, technology & competitive aspects of the emerging industry*, vol. 26. Springer Science & Business Media, 2012.

[2] H. Saboori, M. Mohammadi, and R. Taghe, "Virtual power plant (vpp), definition, concept, components and types," in *2011 Asia-Pacific Power and Energy Engineering Conference*, pp. 1–4, 2011.

[3] E. Dall'Anese, S. S. Guggilam, A. Simonetto, Y. C. Chen, and S. V. Dhople, "Optimal regulation of virtual power plants," *IEEE Transactions on Power Systems*, vol. 33, no. 2, pp. 1868–1881, 2018.

[4] R. W. Kenyon, A. Hoke, J. Tan, and B.-M. Hodge, "Grid-following inverters and synchronous condensers: a grid-forming pair?," in *2020 Clemson University Power Systems Conference (PSC)*, pp. 1–7, IEEE, 2020.

[5] D. Youla, H. Jabr, and J. Bongiorno, "Modern wiener-hopf design of optimal controllers–part ii: The multivariable case," *IEEE Transactions on Automatic Control*, vol. 21, no. 3, pp. 319–338, 1976.

[6] J. Anderson, J. C. Doyle, S. H. Low, and N. Matni, "System level synthesis," *Annual Reviews in Control*, vol. 47, pp. 364–393, 2019.

[7] L. Furieri, Y. Zheng, A. Papachristodoulou, and M. Kamgarpour, "An input–output parametrization of stabilizing controllers: Amidst youla and system level synthesis," *IEEE Control Systems Letters*, vol. 3, no. 4, pp. 1014–1019, 2019.

[8] Y. Zheng, L. Furieri, A. Papachristodoulou, N. Li, and M. Kamgarpour, "On the equivalence of youla, system-level, and input–output parameterizations," *IEEE Transactions on Automatic Control*, vol. 66, no. 1, pp. 413–420, 2020.

[9] Y. Chen and J. Anderson, "System level synthesis with state and input constraints," in *2019 IEEE 58th Conference on Decision and Control (CDC)*, pp. 5258–5263, IEEE, 2019.

[10] M. W. Fisher, G. Hug, and F. Dörfler, "Approximation by simple poles—part i: Density and geometric convergence rate in hardy space," *IEEE Transactions on Automatic Control*, vol. 69, no. 8, pp. 4894–4909, 2024.

[11] M. W. Fisher, G. Hug, and F. Dörfler, "Approximation by simple poles—part ii: System level synthesis beyond finite impulse response," *IEEE Transactions on Automatic Control*, vol. 70, no. 3, pp. 1411–1426, 2025.

[12] Z. Fang and M. W. Fisher, "Hybrid state space and frequency domain system level synthesis for sparsity-promoting $\mathcal{H}_2/\mathcal{H}_\infty$ control design," in *2024 IEEE 63rd Conference on Decision and Control (CDC)*, pp. 8473–8478, 2024.

[13] V. Häberle, M. W. Fisher, E. Prieto-Araujo, and F. Dörfler, "Control design of dynamic virtual power plants: An adaptive divide-and-conquer approach," *IEEE Transactions on Power Systems*, vol. 37, no. 5, pp. 4040–4053, 2021.

[14] C. Scherer and S. Weiland, "Linear matrix inequalities in control," *Lecture Notes, Dutch Institute for Systems and Control, Delft, The Netherlands*, vol. 3, no. 2, 2000.

[15] P. Anderson, A. Fouad, I. of Electrical, and E. Engineers, *Power System Control and Stability*. IEEE Press power engineering series Power system control and stability, Wiley, 2003.

[16] E. D. Andersen and K. D. Andersen, "The mosek interior point optimizer for linear programming: an implementation of the homogeneous algorithm," in *High performance optimization*, pp. 197–232, Springer, 2000.

[17] J. Lofberg, "Yalmip: A toolbox for modeling and optimization in matlab," in *2004 IEEE international conference on robotics and automation (IEEE Cat. No. 04CH37508)*, pp. 284–289, IEEE, 2004.